NASA Technical Memorandum 88852

An Analytical and Experimental Investigation of Resistojet Plumes

Lynette M. Zana and David J. Hoffman
Lewis Research Center
Cleveland, Ohio

and

Loranell R. Breyley and John S. Serafini
University of Akron
Akron, Ohio

Prepared for the
25th Aerospace Sciences Meeting
sponsored by the American Institute of Aeronautics and Astronautics
Reno, Nevada, January 12-15, 1987

NASA

AN ANALYTICAL AND EXPERIMENTAL INVESTIGATION OF RESISTOJET PLUMES

Lynnette M. Zana and David J. Hoffman
National Aeronautics and Space Administration
Lewis Research Center
Cleveland, Ohio 44135

Loranell R. Breyley and John S. Serafini
University of Akron
Akron, Ohio 44325

Abstract

As a part of the electrothermal propulsion plume research program at the NASA Lewis Research Center, efforts have been initiated to analytically and experimentally investigate the plumes of resistojet thrusters. The method of G.A. Simons for the prediction of rocket exhaust plumes is developed for the resistojet. Modifications are made to the source flow equations to account for the increased effects of the relatively large nozzle boundary layer. Additionally, preliminary mass flux measurements of a laboratory resistojet using CO_2 propellant at 298 K have been obtained with a cryogenically cooled quartz crystal microbalance (QCM). There is qualitative agreement between analysis and experiment, at least in terms of the overall number density shape functions in the forward flux region.

This paper also presents estimates of the level of environmental contamination produced by a Space Station resistojet during typical propulsion operations. Predicted number density profiles were used to calculate molecular number column density (NCD) as a function of line-of-sight angle for an observer located at the astronomical observation site of the Space Station. For the case of a resistojet using H_2O propellant, calculated NCD values rise above the proposed requirements for infrared (IR) species in a restricted viewing region representing 20 percent of the total 4π steradian space. In the case of a resistojet operating on a benign mixture (e.g., noninfrared active) of N_2, H_2, He and Ar, quiescent limits on NCD are not exceeded until the observer views along line-of-sight angles which pass near, or look into, the resistojet source.

List of Symbols

A	Simons' plume normalization constant
A_e	nozzle exit area, m^2
A*	throat area, m^2
a_o	sonic velocity at T_o, m/sec
C	capture coefficient
f(θ)	Simons' functional variation of density
M	Mach number
$\dot{m}$	mass flow rate, kg/sec
MW	molecular weight
P	gas pressure, Pa
R	radial distance from centerline or nozzle radius, m
$\bar{R}$	universal gas constant
r	spherical radius, m
S	spherical surface area in space, m^2
T	gas temperature, K
U	gas velocity, m/sec
U_ℓ	limiting velocity of the gas, m/sec
$\bar{U}_\ell$	average limiting velocity of the gas in the boundary layer, m/sec
α	ratio between U_ℓ and $\bar{U}_\ell$
β	plume parameter
γ	specific heat ratio
δ	boundary layer thickness, m
δ*	displacement thickness, m
θ	angle from plume centerline, radians or degrees
θ_o	angle corresponding to the streamline at the edge of the boundary layer, radians or degrees
θ_1	limiting turning angle of the gas at the nozzle exit, radians or degrees
θ_∞	the value of θ_1 for inviscid, supersonic flow, radians or degrees
μ	gas viscosity (as a function of temperature), N sec/m^2
ν	Prandtl-Meyer (P-M) turning angle based on M_e, degrees
ρ	gas density, g/cm^3 or number/cm^3
φ	nozzle half angle, degrees

Sub- or Superscript Notation

*	denotes sonic conditions
e	denotes conditions at the nozzle exit
ℓ	denotes limiting
max	denotes maximum

o denotes stagnation conditions

red denotes reduced effective area

Introduction

The resistojet thruster has been baselined for Space Station auxiliary propulsion applications (Level B Space Station Control Board Directive). It offers low thrust propulsion for drag make-up and also the capability for propulsive, or nonpropulsive, venting of waste gases. Efforts are currently directed toward demonstrating the technology readiness of a long life, multipropellant resistojet for the Space Station.[1-3]

The resistojet concept is relatively simple, as illustrated in Fig. 1. A propellant is passed through a heat exchanger and then expanded through a nozzle to produce thrust. The actual mechanism of heat exchange may be one of convection, conduction, and/or radiation. Potential resistojet propellants include inert gases, water vapor, carbon dioxide, oxygen, cabin air, methane, and hydrogen. Figure 2 presents a photo of an engineering model resistojet designed and fabricated by a Rocketdyne/Technion industrial team under contract to NASA Lewis. The design goals are a 10 000 hr lifetime and a multipropellant capability. Reference 3 provides further details of the design and fabrication of this thruster.

Flow field definition of Space Station propulsion systems and other sources of effluents is of fundamental importance. Of primary concern are the impacts of contamination, both in terms of mass deposition and also environmental contamination. Consequently, designers of the Station core and potential users require definition of the resistojet exhaust in order to assess the plume impacts to Space Station science and technology activities. Other impacts, such as thrust losses or thermal loading caused by plume impingement, may also be of concern depending upon Space Station architecture.

In order to predict possible contamination impacts, the induced environment produced by a resistojet propulsion module needs to be modeled analytically and, where possible, verified experimentally. Both tasks are difficult ones. A detailed numerical treatment of the plume expansion begins prior to the exit of the resistojet nozzle. Although computer codes to analyze the nozzle flow of higher thrust ($\geq$22 N) propulsion devices do exist, the highly viscous nature of resistojets, combined with small nozzle geometries, precludes the immediate adaptation of these codes for the present analysis. Consequently, in order to achieve reasonable analytical results in as timely a manner as possible, it is instructive to begin with source flow analyses of the resistojet exhaust.

G.A. Simons[4] has presented a widely used technique for the prediction of a rocket plume structure. His method is an extension of earlier work by Boynton[5] who used finite difference numerical techniques to analyze an inviscid plume expansion. Viscous boundary layer effects were accounted for in the initial conditions. This paper presents an analysis of the exhaust flow field of a resistojet using Simons' method with slight modifications. The method accounts for the expansion of the supersonic boundary layer of the nozzle, along with the inviscid core. Major plume properties are expressed in terms of conditions at the nozzle exit and in terms of the boundary layer thickness.

In a parallel effort with the analysis, experimental mass flux data have been obtained on a laboratory resistojet using unheated CO_2 as the propellant. A partial mapping of both the forward and back flux regions of the exhaust was conducted using a temperature-compensated, cryogenically cooled quartz crystal microbalance. Preliminary mass flux data are then compared with plume density calculations. Details of the measurement technique and experimental hardware are described.

Lastly, this paper presents estimates of the level of environmental contamination caused by a Space Station resistojet during typical propulsion operations. The assessment is made for a resistojet using H_2O propellant and also a benign gas mixture as the propellant. Predicted levels are compared with proposed Space Station quiescent requirements.

Analyses

Modification of Simons' Method

This section summarizes the development of Simons' technique for plume flow field calculations[4] and the appropriate modifications applicable to resistojet exhaust plumes. A detailed discussion of the rationale and methodology of the following analysis may be found in Ref. 6.

In the far field, rocket nozzle flow may be modeled as a point source. Using continuity, the mass flow in the plume may be written in terms of conditions at the nozzle throat, as

$$\rho^* U^* (\pi R^{*2}) = \iint \rho(r,\theta) U \, dS \qquad (1)$$

It is assumed that the local density $\rho(r,\theta)$ can be be related to its centerline value $\rho(r,\theta = 0)$ by a function $f(\theta)$ such that

$$\rho(r,\theta) = \rho(r,\theta = 0) \quad f(\theta) \qquad (2)$$

Substitution into Eq. (1) gives, upon integration,

$$\rho^* U^* (\pi R^{*2}) = 2\pi r^2 \rho(r,\theta = 0) U_\ell \int_0^{\theta_1} f(\theta) \sin\theta \, d\theta \qquad (3)$$

where θ_1 is the limiting turning angle of the gas. The gas velocity U is removed from the integrand and becomes the limiting gas velocity U_ℓ which is independent of r and θ.

Simons then defines the plume normalization constant A, as

$$A \equiv \left(\frac{U^*}{2U_\ell}\right) \left[\int_0^{\theta_1} f(\theta) \sin\theta \, d\theta\right]^{-1} \qquad (4)$$

where $U_\ell = [\gamma + 1/\gamma - 1]^{1/2} U^*$, based on an isentropic expansion to Mach infinity.

Hence, the local plume density is given by

$$\frac{\rho}{\rho^*} = A \left(\frac{R^*}{r}\right)^2 f(\theta) \qquad (5)$$

The plume structure based on this far field approximation is illustrated in Fig. 3. As shown, the plume is divided into two, axisymmetric regions: the region which originates from the inviscid core of the nozzle, and the region which originates from the supersonic boundary layer. The angle θ_0 corresponds to the streamline at the edge of the boundary layer. The boundary layer is treated as supersonic in this analysis. (It should be noted that preliminary results with a three-dimensional, Navier-Stokes numerical solution of low Reynolds number nozzle flow have indicated that a portion of the nozzle may contain subsonic flow. However, the code is not sufficiently developed for incorporation into the present analysis which is meant to serve as a starting point for analyses of low thrust, electrothermal thrusters.)

Simons determined that the appropriate selections of $f(\theta)$ are:

$$f(\theta) = \left[\cos\left(\frac{\pi}{2}\frac{\theta}{\theta_\infty}\right)\right]^{2/\gamma-1} \qquad \text{for } 0 \le \theta \le \theta_0 \qquad (6)$$

and

$$f(\theta) = f(\theta_0)\exp[-\beta(\theta - \theta_0)] \qquad \text{for } \theta_0 \le \theta \le \theta_\infty \qquad (7)$$

where θ_∞ is the value of θ_1 for an inviscid, supersonic flow. In order to define the density contours as given by Eqs. (5) to (7), the values of the plume constant A, the parameter β, and the angle θ_0 must first be calculated. It will be shown that θ_0 and β are functions of the nozzle exit conditions and boundary layer thickness.

The plume normalization constant requires further consideration. If the nozzle mass flow were to undergo an inviscid expansion, the distribution in the plume would follow the cosine law as given in Eq. (6). Hence, substitution of Eq. (6) into Eq. (4) gives the constant A in terms of γ and θ_∞ as

$$A = \left(\frac{\gamma + 1}{\gamma - 1}\right)^{1/2} \frac{\pi^2}{8\theta_\infty^2} \qquad (8)$$

where the approximation $\sin\theta \sim (2\theta_\infty/\pi)\sin(\pi/2\ \theta/\theta_\infty)$ is used to simplify the evaluation of the integral. This approximation is valid unless the integrand becomes negligibly small.

Next, the angle θ_0 and the parameter β are estimated. Following Simons' analysis, the boundary layer mass flow may be related to the mass flow in the plume that is diverging at angles greater than θ_0 to yield

$$\rho_e U_e \pi \left(2R_e\delta - \delta^2\right) = 2\pi\bar{U}_\ell \int_{\theta_0}^{\theta_\infty} \rho r^2 \sin\theta\, d\theta \qquad (9)$$

where δ is the boundary layer thickness. It is assumed that the displacement thickness is small in comparison to δ. The above equation differs from Simons' basic equation only in the retention of the δ^2 term. Simons neglected this higher ordered term because he was investigating rocket nozzle flow with very small boundary layers (i.e., $\theta_0 \to \theta_\infty$). In resistojet plume analysis this term is not negligible because, in many cases, the boundary layer may make up a considerable portion of the nozzle volume. As a result of the velocity profile in the nozzle boundary layer, it should be noted that, in the plume boundary layer region, there is more than one limiting velocity such that U becomes $\bar{U}_\ell$ upon its removal from the integral. ($\bar{U}_\ell = \alpha U_\ell$ where $0.5 < \alpha < 1.0$ for the supersonic boundary layer.)

Initially, the boundary layer mass flow may be treated as inviscid in order to find the value for the streamline denoted by the angle θ_0. Thus, Eq. (6) is used in Eq. (9) to give

$$f(\theta_0) = \left[\cos\left(\frac{\pi}{2}\frac{\theta_0}{\theta_\infty}\right)\right]^{2/\gamma-1} = \left[\left(\frac{2\delta}{R_e}\right) - \left(\frac{\delta}{R_e}\right)^2\right]^{2/\gamma+1} \qquad (10)$$

Again, an approximation for $\sin\theta$ is used to simplify evaluation of the integral. This gives the following expression for θ_0,

$$\frac{\theta_0}{\theta_\infty} = \frac{2}{\pi}\cos^{-1}\left\{\left[\left(\frac{2\delta}{R_e}\right) - \left(\frac{\delta}{R_e}\right)^2\right]^{\gamma-1/\gamma+1}\right\} \qquad (11)$$

The true situation is that the boundary layer mass flow undergoes an inviscid expansion with its initial conditions specified by a viscous profile. Hence, Eq. (7) is used in Eq. (9) to give

$$\frac{1}{2A}\left[\left(\frac{2\delta}{R_e}\right) - \left(\frac{\delta}{R_e}\right)^2\right]^{\gamma-1/\gamma+1} \left(\frac{\gamma - 1}{\gamma + 1}\right)^{1/2} \frac{U_\ell}{\bar{U}_\ell} = \frac{\left[e^{+\beta(\theta_0 - \theta_\infty)}(-\beta\sin\theta_\infty - \cos\theta_\infty) + \beta\sin\theta_0 + \cos\theta_0\right]}{\beta^2 + 1} \qquad (12)$$

The above equation may be simplified somewhat by assuming $e^{-\beta\theta_\infty} \to 0$ ($\beta > 1$) to give a simple quadratic equation for the parameter β,

$$\beta^2 - \left[\frac{\sin\theta_0}{K}\right]\beta + \left[1 - \frac{\cos\theta_0}{K}\right] = 0 \qquad (13)$$

where

$$K = \frac{1}{2A}\left[\frac{\gamma - 1}{\gamma + 1}\right]^{1/2} \frac{U_\ell}{\bar{U}_\ell}\left[\left(\frac{2\delta}{R_e}\right) - \left(\frac{\delta}{R_e}\right)^2\right]^{\gamma-1/\gamma+1}$$

It should be noted that Eqs. (10) to (12) reduce to that of Simons upon application of his simplifying assumptions for the case of small boundary layer nozzle flow.

Calculations of Nozzle Flow Conditions

The effects of the displacement thickness δ^* in reducing the actual area ratio of the nozzle are accounted for in this analysis. Reasonable estimates of the values of both the displacement thickness and also the boundary layer thickness may be obtained through an application of the Cohen-Reshotko method (Ref. 7). The corresponding reduced Mach number at the nozzle exit is then calculated from a one-dimensional, isentropic, ideal flow analysis based on $(A_e/A^*)_{red}$. Similarly, standard ratios in terms of γ and M_e are used to estimate the gas exit velocity and the stagnation pressure. The exit velocity is dependent upon gas type (γ), stagnation temperature (T_o), and nozzle geometry [(M_e) and $(A_e/A^*)_{red}$].

$$U_e = M_e \left[1 + \frac{(\gamma - 1)}{2} M_e^2\right]^{-1/2} \left[\gamma \frac{\bar{R}}{MW} T_o\right]^{+1/2} \qquad (14)$$

Also, for any given mass flow rate $\dot{m}$ and stagnation temperature T_o, the stagnation pressure is

$$P_o = \left(\frac{\dot{m}}{A_e}\right)\left(\frac{\bar{R}}{MW}\right)\left(\frac{P_o}{P_e}\right)\left(\frac{T_e}{T_o}\right)\left(\frac{a_o}{U_e}\right)\left(\frac{T_o}{a_o}\right) \qquad (15)$$

Lastly, the limiting turning angle of the flow θ_∞, is defined as the difference between the maximum Prandtl-Meyer angle ($M_e \to \infty$) and the P-M angle for the actual M_e plus the half angle of the nozzle. Rather,

$$\theta_\infty = \nu_{max} - \nu + \phi \qquad (16)$$

In this simplified model, then, the included angles $2\theta_o$ and $2\theta_\infty$ encompass the inviscid core and boundary layer regions of the plume, respectively. There is no provision for flow going beyond the limiting angle θ_∞.

Calculation of Plume Number Column Densities

The induced environment produced by a resistojet propulsion module can be analyzed to predict possible contamination which may affect Space Station sensitive surfaces and attached payload optical experiments. The parameters associated with quantifying the induced environment include: (1) number column density (NCD) - the molecular number density integrated along a given line-of-sight; (2) backflow - flow turning through angles greater than 90° from the nozzle centerline; (3) return flux - contaminant molecules impinging on a surface due to intermolecular collisions with ambient molecules; and (4) particle emission. In order to evaluate the impact of these parameters, the exhaust plume density field must first be defined. This report presents only a number column density assessment for a Space Station resistojet. A more complete assessment of the impact of resistojets on Station science and technology activities can be found in Ref. 8.

Number column density (NCD) is the number of molecules per unit area seen by an observer along a specified viewing direction, or line-of-sight (LOS). Column densities can be determined analytically by integrating the plume number density along a LOS from the observer location to infinity. A realistic operational scenario is illustrated in Fig. 4. The observer (from which the LOS originates) is located at the center of the upper boom of the dual keel reference configuration at a point 50 m above the transverse boom. The resistojet source is located at the end of a truss, perpendicular to and 35 m away from, the transverse boom. The observer and the resistojet are in the same spatial plane; consequently, this represents a worst case situation.

The resistojet thruster is assumed to operate under typical conditions, e.g., using Station waste fluids/gases as propellent. The Space Shuttle's fuel cells produce waste water which can be scavenged and used on the Station for propulsion. Therefore, column density calculations for a resistojet using steam as the propellant under both hot (1000 °C) and cold (300 °C) flow conditions are of interest and will be presented. Also, the Environmental Control/Life Support System (ECLSS), Material Technology Labs (MTL), and Attached Payloads (AP) are sources of waste gases which will be collected by a Space Station Waste Fluid Management System and are available for use by the resistojet propulsion module as a mixture of gases. An assessment of the column densities produced by a typical mixture of helium, hydrogen, nitrogen, and argon will also be given.

Apparatus

Instrumentation

Quartz Crystal Microbalances (QCMs) have been used in similar investigations as a means of mapping exhaust flow fields.[9-14] Basically, the QCM used in this study consists of a matched pair of precision 15 MHz quartz crystals. The optically polished crystals are cryogenically cooled to temperatures sufficient to collect mass on one of the crystals (sensor crystal). The other crystal serves as a reference. The QCM translates a change in the beat frequency between the two crystals to mass loading. Sensitivity of the device is 1.56×10^{-9} g/cm^2 Hz. Pertinent details of the QCM are given in Table 1 while a close-up of the device is shown in Fig. 5.

The quartz crystals are seated inside a gold-plated, copper heat sink as shown in the photo. Only the sensor crystal is exposed to mass flow. The QCM heat sink is cooled to -196 °C (77 K) with a continuous flow of liquid nitrogen (LN_2) through the aluminum mounting bracket. A thermal break made of laminated plastic (G-10, not shown in the figure) protects the electronics housing of the QCM from the extreme temperature of the heat sink. The crystals may be set to a desired temperature with a control unit. The available set temperatures range from near heat sink level (as cold as possible) to a temperature 80° above that of the heat sink (using the QCM internal heater). The output of the QCM is sent to a frequency counter.

Resistojet Thruster

Also shown in Fig. 5 is the laboratory resistojet used in this study. The main body of the resistojet is made of Inconel® while the internal heating element is grain-stabilized platinum. Although it is possible to supply approximately 150 W of power to the heater, the mass flux measurement experiments described here-in consist solely of cold flow thruster operation. Carbon dioxide was chosen as the propellant because of its potential usage for Space Station propulsion and because the gas can condense at the LN_2 temperatures. The mass flow rate was 0.20 g/sec at 298 K. This corresponds to a thrust level of 0.12 N (28 mlbf). Further information on the thruster characteristics and operating conditions can be found in the first portion of Table 2.

Figure 5 also points out an obvious difficulty with the use of intrusive probe techniques for local, near field measurements of the resistojet exhaust. Quite often, the extremely small nozzle geometry precludes the use of many probe types in the vicinity of the thruster exit. The QCM and mounting bracket did cause a disturbance to the exhaust flow at some measurement locations; however, because the heat sink and bracket surfaces were maintained at the saturation temperature of LN_2, it can be assumed that the greater portion of CO_2 mass flux hitting the surfaces condensed on them, thereby reducing the disturbance.

Test Facility and Experimental Set-Up

The mass flux measurements were conducted in the 4.6 m (15 ft) diameter vacuum facility at NASA Lewis. The vacuum tank has a 4.2 m inner working diameter and is 19 m long. The tank was chosen for its size and pumping capacity. It is equipped with a pumping train consisting of 20 oil diffusion pumps, backed by four rotary blowers and four rotary piston vacuum pumps. The tank is also equipped with a LN_2-cooled condensor which lines the major portion of the inner tank wall for added pumping capability. For the resistojet mass flow the specified earlier, the tank maintained a background pressure of 2.7×10^{-3} Pa (2×10^{-5} torr).

The cryogenically cooled QCM and the resistojet were mounted on radial positioning arms as shown in Fig. 6. The two arms were rigidly attached at the end of push/pull rods that extended the assembly into the main tank area through a 0.9 m (36 in.) diameter port entrance as shown in the figure. A retractable aluminum tray supported the two axial positioning rods on a moveable test cart. The arms could rotate radially through a 90° arc (±45° with respect true vertical); similarly, the push/pull rods could be positioned axially to permit a mass flux mapping of one quadrant of the assumed axisymmetric exhaust. Electronic inclinometers attached at the end of the push/pull rods were used to mark the location of the arms with respect to the true vertical position. Because the tank LN_2 baffles were in use during the experiments, the sensitive electronics of the QCM and inclinometers were kept operational by wrapping them with resistive heating tape.

Procedure

Prior to each mass flux experiment, the positions of the QCM and the thruster were calibrated for the region of exhaust to be surveyed. Additionally, cooldown of the large vacuum tank baffles was initiated at least 15 hr before each test. The temperatures of several critical baffle locations were monitered throughout the duration of the test period to ensure a near-equilibrium tank background condition.

The experimental assembly was installed in the 0.9 m diameter belljar entrance to the tank. The QCM sensor was internally heated to +90 °C for a period of about 20 min to clean the sensor crystal of possible contaminants. Once this was completed, the axial positioning rods holding the QCM and thruster were carefully extended into the main tank area and cooldown of the QCM was begun. This cooldown generally took 1 to 1-1/2 hr. The QCM heat sink was cooled to -196 °C and then maintained at this temperature with a continuous flow of LN_2 through the aluminum mounting bracket. A 150 liter (40 gal) dewar supplied the LN_2 at 140 to 310 KPa (20 to 45 psia). The QCM sensor was set to a desired temperature with the control unit. Once the sensor and the heat sink had stablized at desired temperatures, background mass flux data (e.g., no thruster flow) were taken for a period of 30 min or longer. Typically, the background mass flux decreased slightly during the test period so it was rechecked periodically. The background mass flux was usually 2 to 3 percent of the centerline flux during thruster operation.

Back flux Measurements

Back flux measurements were conducted to find the percentage of mass flow turning through angles greater than 90° from the thruster centerline and also the limiting turning angle. The mounting arrangement for the QCM on its positioning arm did not permit in-situ rotation of the QCM sensor into the flow streamlines. However, it was possible to orient the QCM in three different positions: (1) with the plane of the QCM sensor crystal perpendicular to the thruster centerline; (2) with the sensor crystal plane at 135° from the thruster centerline; and (3) with the sensor plane 180° to the thruster exit plane to determine back-scatter effects. For the back flux measurements, the QCM temperature control was set so that the sensor reached its lowest possible temperature (-189.6 °C) to ensure condensation of the CO_2. Deposition rates were measured with the QCM oriented in all three of the above-mentioned positions.

Forward Flux Measurements

The QCM used in this study had a limited dynamic loading capability. High flux rates or rapid changes in the flow pattern would cause the sensor to be overloaded. This overload would generally be characterized by an exponential rise in the frequency output to approximately 8 to 10 kHz where the signal disappeared. The limitations of the QCM dynamic response and also the physcial limitations imposed by the measurement apparatus precluded the measurement of CO_2 deposition rates in the forward flux region. However, the CO_2 propellant did contain a small percentage of water

(220 parts per million as measured by the dew point method). In order to get some estimate of the forward flux density distribution, the H_2O was used as a tracer. Inherent to this measurement technique are the assumptions that: the concentration of H_2O was uniform throughout the propellant; H_2O (and only H_2O) condensed on the sensor crystal; and the water molecules expanded in direct correspondence to the CO_2, at least in the near continuum region of the measurements.

The QCM sensor temperature was set at -175 °C so that it would condense the H_2O mass flux but not the CO_2. The QCM control unit was able to maintain this temperature to within ±0.1 °C for most measurement locations. Mass flux surveys were taken with the water tracer method at axial stations of 36.4 and 58.8 cm downstream of the thruster. The QCM sensor crystal was oriented parallel to and facing the nozzle exit plane.

The usual test procedure involved moving the QCM and thruster to initial measurement locations (usually at a radial distance of at least 50 cm from one another), establishing a background mass flux rate on the sensor, and then beginning propellant flow through the thruster. Data were taken at 1 min time intervals, recording the QCM beat frequency output, the heat sink and sensor temperatures, as well as the temperatures of all sensitive electronics. Generally, the QCM data were taken for a period of at least 5 to 10 min at any one location before moving to a new one. Because of the limited dynamic loading capability of the QCM, it was easier to move the thruster with respect to the QCM rather than vice versa so this was done where possible. Nonetheless, it usually took several minutes to re-establish a stable frequency output whenever the QCM was subjected to any change in the flow pattern.

Interpretation of Results

The QCM beat frequency output, when monitored over a period of time, could be directly converted to a mass flux measurement (g/cm^2 sec). In order to convert the measured mass flux to a CO_2 number density, the values of two important parameters must be obtained. The first parameter is the gas velocity at the location of interest. Measurements of a simulated rocket exhaust plume[15] have shown that the gas velocity exponentially decreases away from the thruster centerline to a value which is one half of the exit velocity at the limiting turning angle θ_∞. A similiar relationship for the CO_2 velocity may be obtained, as

$$U(\theta) = U_e \exp(-0.0077\,\theta) \qquad (17)$$

where U_e is the gas exit velocity determined by Eq. (14) and the angle θ is in degrees.

The second parameter is the Capture Coefficient, C. It is defined as the fraction of particles impinging on a surface which are trapped by the surface after the collision.[16] Measurements of the Capture Coefficients of gases on cryogenic surfaces have been made specifically for cryopumping applications.[16-18] Here, the primary concern is with a random flux deposition which is dependent upon an average gas temperature; hence, the capture coefficient was assumed to be independent of the rate of incidence on the surface.[17] The measured values of C for both carbon dioxide and water as a function of gas temperature may be found in Table 3. In the case of directed flux deposition, as in the present case, it seems likely that not only will some of the incident particles reflect off the surface after the collision, but also some of the particles already trapped by the surface may be desorbed by the action of impingement. Specific experiments to determine the extent of this effect can be performed; however, due to the preliminary nature of the mass flux data presented here, the measured values of C at 300 K found in Table 3 will be used in the data reduction.

Results and Discussion

This section presents results of the analytical and experimental investigation of the resistojet plume. First, the source flow equations developed earlier are applied to a laboratory resistojet using unheated CO_2 as the propellant. Mass flux data taken with a cryogenically cooled quartz crystal microbalance are converted to number density profiles for comparison. The upper portion of Table 2 lists the major characteristics and operating conditions of the laboratory resistojet for both analysis and experiment. This section also presents estimates of the level of environmental contamination caused by a Space Station resistojet during propulsion operations. Table 4 lists the major characteristics and operating conditions of the Space Station resistojet using H_2O propellant and also a benign mixture as the propellant. Comparisons are made between predicted number column density levels and proposed quiescent requirements.

Calculations of the Laboratory Resistojet Exhaust Flow Field

Calculated nozzle exit conditions and plume properties of the laboratory thruster are given in the lower portion of Table 2. For the flow conditions specified, the calculated boundary layer comprises over 40 percent of the cross-sectional area at the nozzle exit. The calculated exit velocity is 634 m/sec. It should be mentioned that this value compares well with a measured value of 627 m/sec, based on thrust measurements of this same thruster under similar flow conditions.[19] The resultant exhaust flow field is shown in Fig. 7. Plotted in the figure are lines of constant CO_2 number density emanating from the resistojet source. The dashed lines in the figure denote the calculated angles θ_o and θ_∞ at 28° and 90°, respectively. The sharp fall-off in number density away from the thruster centerline demonstrates the relatively benign nature of resistojet operation in that its greatest impact will be in a very confined region of space directly downstream of the thruster. Mass flow calculations based on these density contours indicate that the inviscid core region of the plume comprises 60 percent of the total mass flow while 75 percent of the flow is within a symmetrical cone of half angle 35° and 96 percent of the flow is contained within 60°.

Comparison with Preliminary Mass Flux Measurements

Figure 8 presents a close-up of the above calculated flow field along with experimental mass flux data taken with the QCM. The temperature of the crystals was set as cold as possible so that

CO_2 deposition rates were measured. The symbols in the figure mark the location of the QCM and the flat portion of each symbol denotes the orientation of the sensor crystal with respect to the thruster exit. The dashed line in Fig. 8 indicates the zone where measurements could be obtained.

An accurate measurement of the background CO_2 number density in the vacuum tank (e.g., no thruster flow) is critical to the back flux measurements. Because the vacuum facility environment reflected its previous experience, it was necessary to take background data immediately prior to each data set. For the data displayed in Fig. 8, the measured background mass flux rate was consistently between 0.8×10^{-11} and 1.1×10^{-11} g/cm^2 sec. This represents an average CO_2 background number density of $(6 \pm 1) \times 10^7$ molecules/cm^3. It is felt that the background measurements reflect a true condition of the vacuum environment (and not an inherent drift in the QCM frequency output) because: (1) the vacuum tank condition was in, to the extent feasibile, a near-equilibrium condition; (2) both the QCM sensor and heat sink were thermally stable; (3) the QCM beat frequency increased at a constant rate over a long period of time; and (4) changes in the QCM output always reflected noticeable changes in the tank environment (e.g., change in baffle temperature, etc.)

The back flux measurements with CO_2 collection yielded results as summarized in Table 5. With the plane of the QCM sensor facing perpendicular to the thruster centerline (Test Number 29 data), no significant increase in the deposition rate above the background occurred when flow was introduced through the thruster. For all but one of the measurement locations, no portion of the sensor crystal area was in direct line of sight of the edge of the nozzle lip. Conversely, when the QCM sensor was off-set 45° from the thruster exit plane (Test Number 34 data), the QCM dynamic response was exceeded at locations corresponding to angles of 87°, 93°, and 97° as measured from the thruster centerline. However, at a position corresponding to an angle of 99°, the mass flux rate decreased sharply to a measureable level which was just slightly above the background. It should be noted that, at this measurement location, 54 percent of the crystal area is still within direct line of sight of the edge of the nozzle lip. These CO_2 collection data seem to indicate that the flow is travelling along a straight path (i.e., free molecular flow). Further, and perhaps more importantly, the sharp decrease in density between 97° and 99° suggests a definite boundary to the greatest portion of the mass flux (>99 percent), but one which is beyond the calculated limiting angle, $\theta_\infty = 90°$. This discrepancy can be accounted for, in part, by an actual displacement thickness larger than that used in the analysis. Further, numerical calculations using Direct Simulation Monte Carlo (DSMC) techniques have determined that flow in the free molecular region of the exhaust is dependent upon the flow angle at the nozzle lip and also species molecular weight.[20-22] A detailed numerical treatment of the plume, such as a combination of the Method of Characteristics and the DSMC methods, is necessary to accurately model and assess the back flux.

An attempt was made to measure CO_2 deposition rates in the forward flux region of the exhaust (Test No. 30). The QCM was located at a position 36.3 cm downstream of the thruster exit at a radial distance of 50.0 cm. The sensor crystal was parallel to and facing the thruster. Because of the extremely high flux rates, the dynamic response of the QCM was exceeded at this location. Consequently, only an estimate of the minimum value of the actual CO_2 number density can be made. The value, $\rho \geq 2 \times 10^{10}$ molecules/cm^3, can neither support nor refute the calculated flow field distribution in the forward flux region.

Mass Flux Measurements Using H_2O as a Tracer

In the forward flux region of the resistojet exhaust, mass flux data were taken using H_2O as a tracer of the CO_2 propellant. The measurements were made along the radii at two specific axial stations downstream of the thruster, at $x = 36.4$ and 58.8 cm. The CO_2 mass flux profiles at the two stations are presented in Figs. 9(a) and (b). The data are plotted as a function of angle off centerline. Comparisons of the experimental data with calculated density profiles are shown in Figs. 10(a) and (b). The data points are curve-fit to the calculated profile at a midrange measurement location ($\theta = 27.5°$) in Fig. 10(a). The same correction factor is used in Fig. 10(b). The QCM data, based on a concentration of water at 220 parts per million in the CO_2, were actually lower than the predicted values by a factor of 3.5. This discrepancy could be the result of a systematic error in either the experimental technique or the analysis. However, the fact that the theory and data are in good agreement in terms of an overall shape function of the density profile gives some confidence to both the experimental and analytical techniques. A complete summary of the forward flux QCM data is given in Table 6.

Number Column Density Assessment of a Space Station Resistojet

Calculated Number Column Densities as a function of line-of-sight angle for the Space Station scenario described previously are presented in Figs. 11 and 12. The observer zenith (Fig. 4) is located at an angle of 0° while the resistojet source is at 145°. Also shown in the figures are the proposed number column density requirements which must not be exceeded for all lines-of-sight. (It should be noted that there are no NCD requirements during nonquiescent periods.)

The column density requirements for infrared active molecules, such as H_2O, is 10^{11} molecules/cm^2. The NCDs for a resistojet using H_2O propellant remain relatively low in comparison with the requirement until the observer begins to look aft. As shown in Fig. 11, the NCDs rise steadily until they exceed the proposed limit at about 45° aft of zenith, and then begin an exponential rise toward infinity for the LOS intersecting the resistojet source. Although not shown in the figure, the NCDs will drop rapidly once past the source to a relatively low level. It should be mentioned that lines of sight greater than 90° are presumed to be seldom used viewing directions for sensitive optical instruments located on the astronomical platform because the instruments will "see" a greater NCD due to the natural atmosphere than that imposed by the thruster. Further, line-of-sight angles which pass near the Space Station structure will tend to be avoided by sensitive optical instruments.

Nonetheless, the obvious disparity between calculated NCD values and the proposed limits indicates that a resistojet should not use H_2O propellant during quiescent periods if observations are to be made along LOS angles between 45 and 150°. It should be mentioned here that the solid angle subtended by this restricted viewing region represents only 20 percent of the total 4π steradian viewing space.

For the case of a resistojet operating on a benign gas mixture (Fig. 12), the NCD curve shows the same general shape function with LOS angle as the H_2O resistojet. But, since none of the molecules in the gas mixture are infrared active, the limits for molecules of this type are less stringent, at 10^{13} molecules/cm^2. The figure presents NCD curves for three specific operational thrust levels. For a thrust level of 0.4 N (100 mlb_f), the quiescent requirements on NCD are not exceeded until the observer views along LOS angles which pass near, or look into, the resistojet source.

Concluding Remarks

The resistojet thruster is currently baselined for Space Station auxiliary propulsion needs. Definition of the resistojet flow field is required in order to assess the exhaust plume impacts to Station science and technology activities. This paper has presented initial efforts in an analytical and experimental investigation of resistojet plumes. Firstly, a modified version of Simons' source flow technique for the prediction of exhaust flow fields was developed for the resistojet thruster. The increased effects of the relatively large nozzle boundary layer characteristic of resistojet nozzle flow were accounted for in the analysis. In a parallel effort, mass flux measurements of a laboratory resistojet operating on unheated CO_2 propellant were obtained using a cryogenically cooled quartz crystal microbalance. There is qualitative agreement between theory and experiment, at least in terms of the overall density shape functions in the forward flux region. Further, the QCM data indicated that flow does go beyond the calculated limiting turning angle (90° for the laboratory resistojet) but the amount represents only very small fraction of the total thruster throughput.

This paper has also presented the application of Simons' method to a Space Station resistojet using H_2O propellant and also a mixture of gases as the propellant. The predicted number density profiles were used to calculate molecular number column density as a function of line-of-sight angle for an observer located at the astronomical observation site on the Space Station. For the case of a H_2O resistojet, calculated NCD values rise above the proposed requirements for infrared (IR) species when the observer looks between 45 and 150° aft of zenith. This restricted viewing region represents only 20 percent of the total 4π steradian viewing space. However, it is not recommended that H_2O propellant be used during quiescent periods if these viewing angles are required by an observer. In the case of a resistojet using a benign (e.g., noninfrared active) propellant mixture, quiescent limits on NCD are not exceeded until the observer looks at LOS angles which pass near, or look into, the resistojet source.

Acknowledgements

The authors gratefully acknowledge the assistance of Dr. Benny R. Riley of the University of Evansville for his participation and assistance in technical discussions concerning the theoretical analysis of this work.

References

1. Jones, R.E., "Space Station Propulsion: The Advanced Development Program at Lewis," AIAA Paper 85-1154, July 1985.

2. Morren, W.E., Whalen, V.V., Sovey, J.S., "Performance and Endurance Tests of a Multipropellant Resistojet for Space Station Auxiliary Propulsion," AIAA Paper 86-1435, June 1986.

3. Pugmire, T.K., Cann, G.L., Heckert, B., Sovey, J.S., "A 10,000 Hour Life Multipropellant Engine for Space Station Applications," AIAA Paper 86-1403, June 1986.

4. Simons, G.A., "Effect of Nozzle Boundary Layers on Rocket Exhaust Plumes," AIAA Journal, Vol. 10, No. 11, Nov. 1972, pp. 1534-1535.

5. Boynton, F.P., "Exhaust Plumes from Nozzles with Wall Boundary Layers," Journal of Spacecraft and Rockets, Vol. 5, No. 10, Oct. 1968, pp. 1143-1147.

6. Hoffman, D.J., "Prediction of the Space Station Induced Environment Resulting From Resistojet Exhaust Plumes," Master's Thesis, Case Western Reserve University, to be published.

7. Cohen, C.B., and Reshotko, E., "The Compressible Laminar Boundary Layer with Heat Transfer and Arbitrary Pressure Gradient," NACA Report No. 1294, 1956.

8. Hoffman, D.J., "Space Station Environmental Contamination Resulting from Resistojet Exhaust Plumes," NASA PIR No. 125, Lewis Research Center, Jan. 1986.

9. Bailey, A.B. and Price, L.L., "Flow Field Mapping of Carbon Dioxide Nozzle Expansion into Vacuum," AEDC-TR-85-26, July 1985.

10. Williams, W.D., McCay, T.D., Powell, H.M., and Weaver, D.P., "Experimental Study of the Plume Characteristics of an Aged Monopropellant Hydrazine Thruster," AEDC-TR-79-2, Apr. 1979.

11. Alt, R.E., Powell, H.M., Price, L.L., Frazine, D.F., and Stephenson, W.B., "Contamination Measurements from a 5 lb_f Thrust Bipropellant Engine - Phase II," AEDC-TSR-79-V4, Jan., 1979.

12. Chirivella, J.E., "Molecular Flux Measurements in the Back Flow Region of a Nozzle Plume," Jet Propulsion Laboratory, Pasadena, CA, JPL-TM-33-620, July 1973. (NASA CR-133602)

13. Chirivella, J.E., "Hydrazine Engine Plume Contamination Mapping," AFRPL-TR-75-16, Oct. 1975.

14. Chirivella, J.E., "Mass Flux Measurements and Correlations in the Back Flow Region of a Nozzle Plume," AIAA Paper 73-731, July 1973.

15. Calia, V.S. and Brook, J.W., "Measurements of a Simulated Rocket Exhaust Plume Near the Prandtl-Meyer Limiting Angle," Journal of Spacecraft and Rockets, Vol. 12, No. 4, Apr. 1975, pp. 205-208.

16. Eisenstadt, M.M., "Condensation of Gases during Cryopumping-The Effect of Surface Temperature on the Critical Energy for Trapping," Journal of Vacuum Science and Technology, Vol. 7, No. 4, 1970, pp. 479-484.

17. Dawson, J.P. and Haygood, J.D., "Cryopumping," Cryogenics, Vol. 5, No. 2, Apr. 1965, pp. 57-67.

18. Brown, R.F. and Wang, E.S.J., "Capture Coefficients of Gases at 77° K," Advances in Cryogenic Engineering, Vol. 10, edited by K.D. Timmerhaus, Plenum, New York, 1964, pp. 283-291.

19. Private Communication with W.E. Morren, NASA Lewis Research Center, Cleveland, OH, Oct., 1985.

20. Chirivella, J.E., Baroth, E.C., and Guernsey, C.S., "Nozzle Lip Flow and Self-Scattering Molecular Collisions as Contributers to Plume Backflow," JANNAF 13th Plume Technology Meeting, edited by T.M. Gilliland, Chemical Propulsion Information Agency, CPIA-PUB-357-Vol-1, 1982, pp. 19-38.

21. Guernsey, C.S., McGregor, R.D., "Bipropellant Rocket Exhaust Plume Analysis of the Galileo Spacecraft," AIAA Paper 86-1488, June 1986.

22. Hueser, J.E., Melfi, L.T., Bird, G.A., and Brock, F.J., "Rocket Nozzle Lip Flow by Direct Simulation Monte Carlo Method," AIAA Paper 85-0995, June 1985.

TABLE 1. - CHARACTERISTICS OF THE QUARTZ CRYSTAL MICROBALANCE (QCM)

Crystal frequency, MHz	10^{15}
Mass sensitivity, g/cm^2 Hz	1.56×10^{-9} Hz
Operational temperature range, °C	-100 to -190 (cryogenically cooled)
Beat frequency output, KHz	1 to 8
Heat sink dimensions, cm	2.92 diam. x 3.94 length
Crystal diameter (exposed), cm	0.851
Crystal area (exposed), cm^2	0.569

TABLE 2. - RESISTOJET NOZZLE GEOMETRY/OPERATING CONDITIONS AND CALCULATED NOZZLE FLOW/PLUME PROPERTIES

Nozzle Geometry	
Throat radius	$R^* = 4.06 \times 10^{-4}$ m
Exit radius	$R_e = 3.81 \times 10^{-3}$ m
Half angle	$\phi = 20°$
Area ratio	$A_e/A^* = 88$
Reduced area ratio[a]	$(A_e/A^*)_{red} = 65$
Thruster Operating Conditions	
Propellant	CO_2
Molecular weight	MW = 44.01
Specific heat ratio	$\gamma = 1.288$
Viscosity (@ 298 K)	$\mu = 15.2 \times 10^{-6}$ N sec/m^2
Mass flow rate	$\dot{m} = 0.20$ g/sec
Stagnation temperature	$T_o = 298$ K
Calculated Nozzle Exit Conditions	
Stagnation pressure	$P_o = 1.39 \times 10^5$ N/m^2
Exit Mach number	$M_e = 5.24$
Exit velocity of the gas	$U_e = 634$ m/sec
Limiting gas velocity	$U_\ell = 710$ m/sec
Average limiting gas velocity	$\overline{U}_\ell = 532$ m/sec ($\alpha = 0.75$)
Boundary layer thickness	$\delta = 7.87 \times 10^{-4}$ m
Displacement thickness	$\delta^* = 5.33 \times 10^{-4}$ m
Plume Properties	
Normalization constant	$A = 1.41$
Parameter beta	$\beta = 4.3$
Angle θ_o	$\theta_o = 28°$
Limiting angle	$\theta_\infty = 90°$

[a]Reduction due to displacement thickness.

TABLE 3. - MEASURED VALUES OF THE CAPTURE COEFFICIENT BASED ON CRYOPUMPING APPLICATIONS

[Surface temperature, 77 K.]

	Gas temperature, K	Capture coefficient
CO_2 [a,b]	195	0.85
	300	.63
	400	.49
H_2O[b]	300	.92

[a]Data from Ref. 17.
[b]Data from Ref. 18.

TABLE 4. - SPACE STATION RESISTOJET NOZZLE GEOMETRY/OPERATING CONDITIONS AND CALCULATED NOZZLE FLOW/PLUME PROPERTIES

Nozzle Geometry

Throat radius, $R^* = 5.09 \times 10^{-4}$ m
Exit radius, $R_e = 5.08 \times 10^{-3}$ m

Half angle, $\phi = 20°$

Geometric area ratio, $A_e/A^* = 100$

	H_2O (T_o = 300 °C)	H_2O (T_o = 1000 °C)	Mixture[a] (H_2,N_2,He,Ar)
Thruster Operating Conditions			
P_o, N/m^2	1.59×10^5	1.65×10^5	3.54×10^5
MW	18.015	18.015	11.98
γ	1.33	1.33	1.47
$\dot{m}$, g/sec	0.113	0.175	0.213
Calculated Nozzle Exit Conditions			
M_e	5.27	5.37	6.57
U_e, m/sec	1972	1329	2243
U_ℓ, m/sec	2179	1458	2355
$\bar{U}_\ell$, m/sec (= 0.75)	1634	1093	1766
δ, m	2.2×10^{-3}	2.0×10^{-3}	1.9×10^{-3}
δ^*, m	1.6×10^{-3}	1.4×10^{-3}	1.5×10^{-3}
Plume Properties			
A	1.63	1.67	2.98
B	3.54	3.76	5.00
θ_0	17°	18°	15°
θ_∞	81°	80°	56°

[a]Benign mixture mole fractions: H_2 (0.455); N_2 (0.193); He (0.234); and Ar (0.119).

TABLE 5. - SUMMARY OF MASS FLUX MEASUREMENTS WITH CO_2 COLLECTION

Test number	QCM/thruster orientation	Angle off centerline, degree	Axial distance, cm	Radial distance, cm	Percent of sensor area exposed,[a] percent	Measured mass flux, g/cm^2 sec	CO_2 number density,[c,d] molecules/cm^3
29	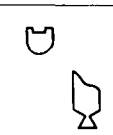	91°	-0.3	13.0	0	1.0×10^{-11}	7.4×10^{7}
		90°	-0.3	50.0	0	7.8×10^{-12}	5.5×10^{7}
		117°	-6.6	13.0	25	1.1×10^{-11}	7.8×10^{7}
		98°	-6.6	50.0	0	1.0×10^{-11}	7.4×10^{7}
30		62°	+36.3	67.1	55	$\geq3.7\times10^{-8}$	$\geq2\times10^{10}$
34	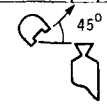	[b]87°	+1.3	25.1	60	$\geq4.6\times10^{-8}$	$\geq3\times10^{10}$
		[b]93°	-1.3	25.1	56	$\geq6.4\times10^{-8}$	$\geq4\times10^{10}$
		[b]93°	-1.3	25.1	56	$\geq4.3\times10^{-8}$	$\geq3\times10^{10}$
		[b]93°	-1.3	25.1	56	$\geq5.0\times10^{-8}$	$\geq4\times10^{10}$
		[b]97°	-3.2	25.1	55	$\geq7.8\times10^{-8}$	$\geq6\times10^{10}$
		99°	-3.8	25.1	54	1.4×10^{-10}	1.0×10^{8}

[a]The percentage of total sensor crystal area which is in a direct line-of-sight of the thruster exit (forward flux) or nozzle lip (back flux); e.g., this value gives a measure of the shadowing effect imposed by the physical surfaces of the QCM heat sink.
[b]QCM overloaded at this location; only an estimate of the absolute minimum CO_2 number density can be made.
[c]The background CO_2 number density for these tests was $(6\pm1)\times10^{7}$ molecules/cm^3.
[d]Tank pressure was 2.7×10^{-3} Pa.

TABLE 6. - SUMMARY OF MASS FLUX MEASUREMENTS WITH H_2O COLLECTION

[Sensor temperature was -175.1 °C.]

Test number	Axial distance, cm	Angle off centerline, deg	Radial distance, cm	Percent of sensor area exposed,[a] percent	H_2O measured mass flux, g/sec cm^2	Velocity U(θ),[b] cm/sec	H_2O number density,[c] number/cm^3	CO_2 number density,[d] number/cm^3
32	36.3	61.3	67.1	50	9.9×10^{-11}	39 500	9.3×10^{7}	4.2×10^{11}
		61.3	67.1	50	7.8×10^{-11}	39 500	7.3×10^{7}	3.3×10^{11}
		54.0	49.8	53	9.4×10^{-11}	41 800	8.3×10^{7}	3.8×10^{11}
		46.0	38.4	59	5.7×10^{-11}	44 500	4.8×10^{7}	2.2×10^{11}
		40.7	31.0	64	1.6×10^{-10}	46 300	1.3×10^{8}	5.9×10^{11}
		35.8	26.4	68	2.7×10^{-10}	48 100	2.1×10^{8}	9.5×10^{11}
		31.8	22.4	72	6.1×10^{-10}	49 600	4.6×10^{8}	2.1×10^{12}
		27.5	19.3	75	1.1×10^{-9}	51 300	7.7×10^{8}	3.5×10^{12}
		22.6	15.2	80	1.5×10^{-9}	53 300	1.0×10^{9}	4.5×10^{12}
		16.7	10.9	85	2.4×10^{-9}	55 700	1.6×10^{9}	7.3×10^{12}
		16.7	10.9	85	2.8×10^{-9}	55 700	1.8×10^{9}	8.2×10^{12}
		5.2	3.3	96	3.3×10^{-9}	60 900	2.0×10^{9}	9.1×10^{12}
31	58.8	37.6	45.2	66	1.7×10^{-10}	47 500	1.3×10^{8}	5.9×10^{11}
		34.6	40.6	69	2.5×10^{-10}	48 600	1.9×10^{8}	8.6×10^{11}
		26.6	29.5	76	5.4×10^{-10}	51 700	3.9×10^{8}	1.8×10^{12}
		22.7	24.6	79	5.9×10^{-10}	53 200	4.1×10^{8}	1.9×10^{12}
		18.9	20.1	83	6.8×10^{-10}	54 800	4.6×10^{8}	2.1×10^{12}

[a]The percentage of total crystal area which is in a direct line-of-sight of the thruster exit (forward flux) or nozzle lip (back flux); e.g., this value gives a measure of the shadowing effect imposed by the physical surfaces of the QCM heat sink.
[b]Gas velocity based on Eq. (15) and U_e = 634 m/sec.
[c]Tank background density (no thruster flow) was 6×10^{7} molecules/cm^3.
[d]Based on measured water concentration of 220 parts per million in the CO_2.

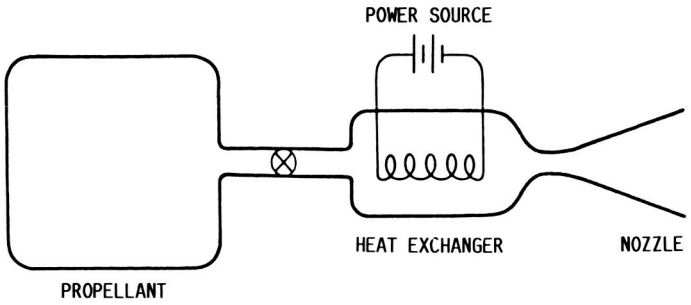

FIGURE 1. - SCHEMATIC OF A RESISTOJET THRUSTER.

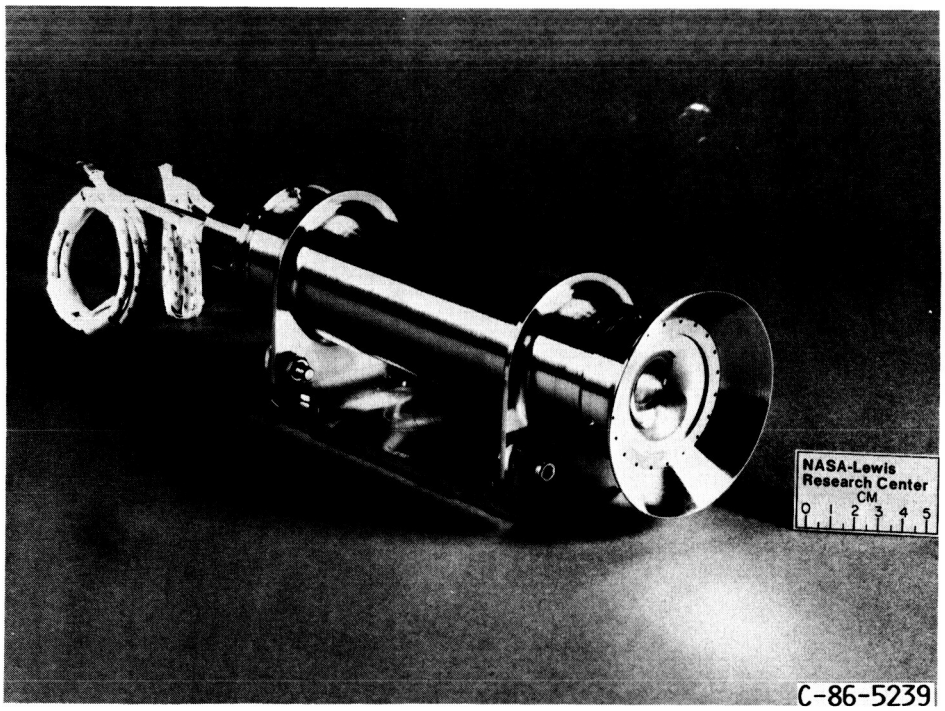

FIGURE 2. - ENGINEERING MODEL RESISTOJET DEVELOPED FOR SPACE STATION APPLICATIONS.

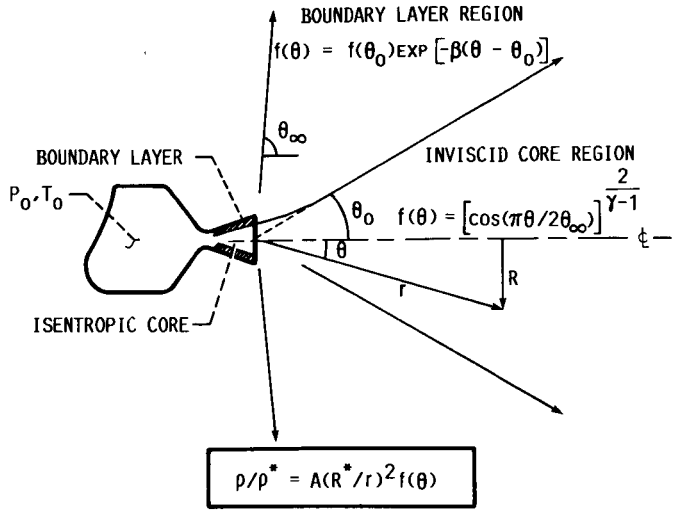

FIGURE 3. - PLUME STRUCTURE BASED ON FAR FIELD APPROXIMATION.

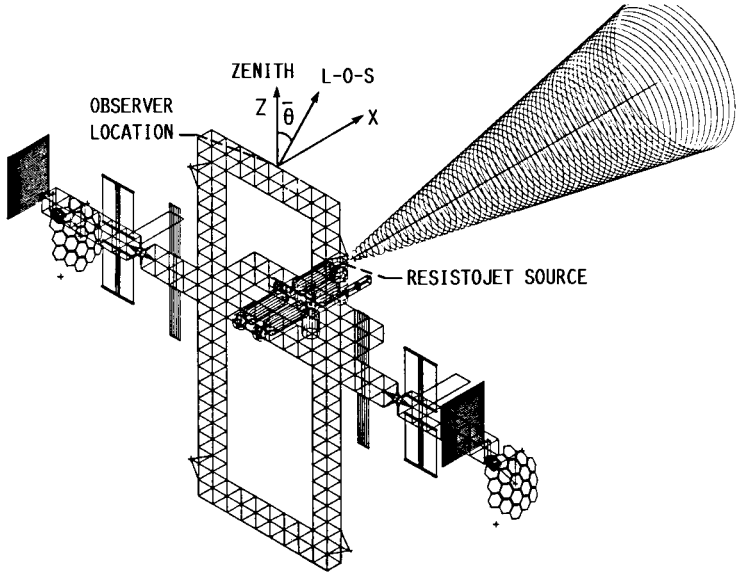

FIGURE 4. - SPACE STATION RESISTOJET OPERATIONAL SCENARIO FOR NUMBER COLUMN DENSITY CALCULATIONS.

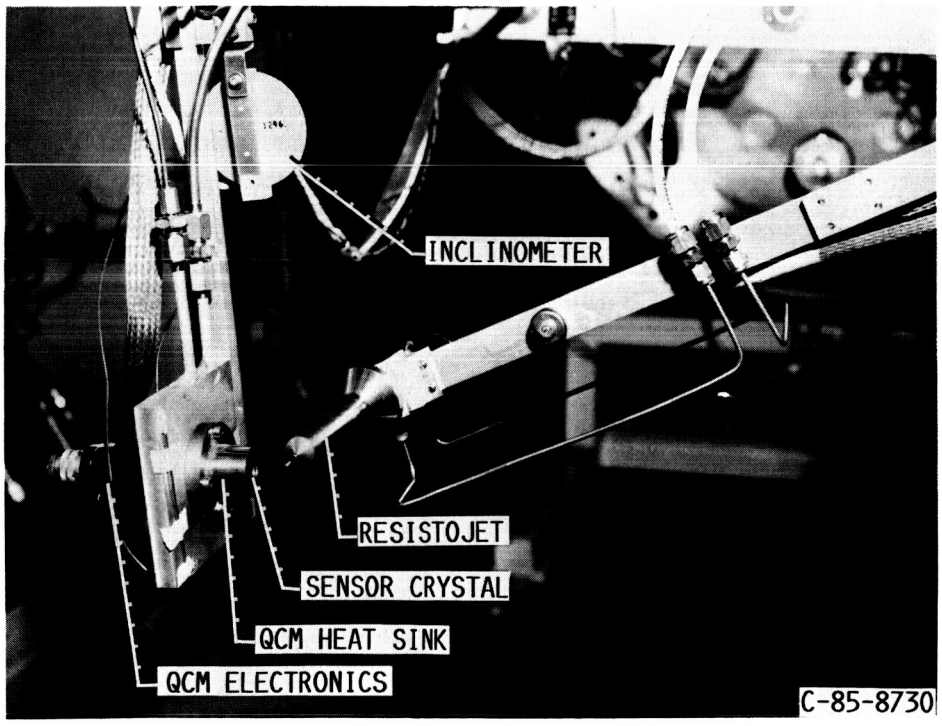

FIGURE 5. - LABORATORY RESISTOJET AND QCM.

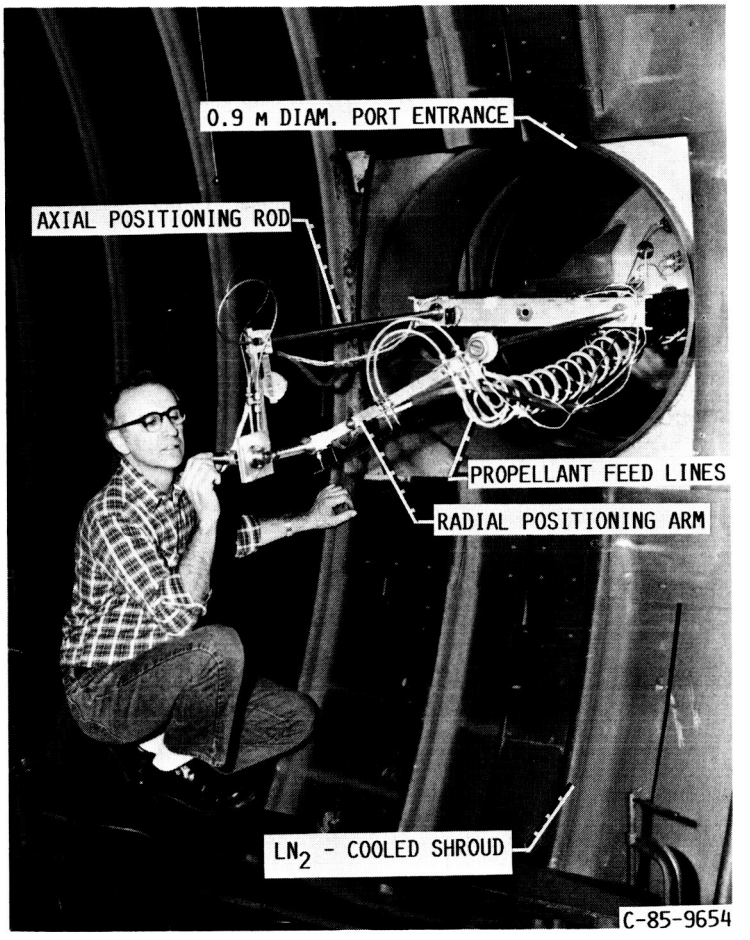

FIGURE 6. - EXPERIMENTAL APPARATUS FOR MASS FLUX MEASUREMENTS.

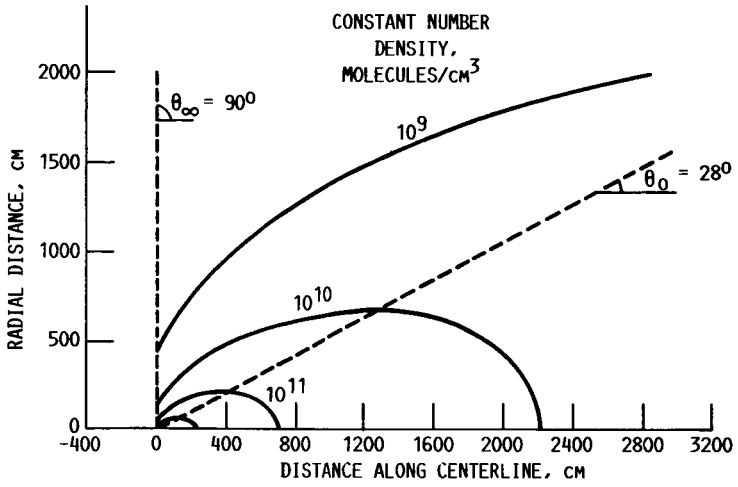

FIGURE 7. - CALCULATED EXHAUST FLOW FIELD OF A CO_2 RESISTOJET. PROPELLANT MASS FLOW RATE, 0.20 G/SEC; T_0 = 298 K.

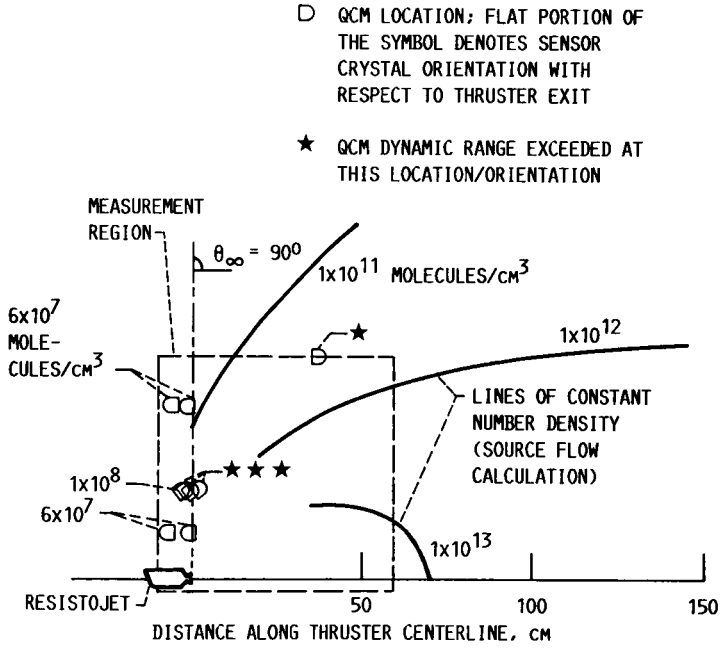

FIGURE 8. - COMPARISON OF EXPERIMENTAL MASS FLUX DATA (CO_2 COLLECTION) WITH SOURCE FLOW PREDICTIONS.

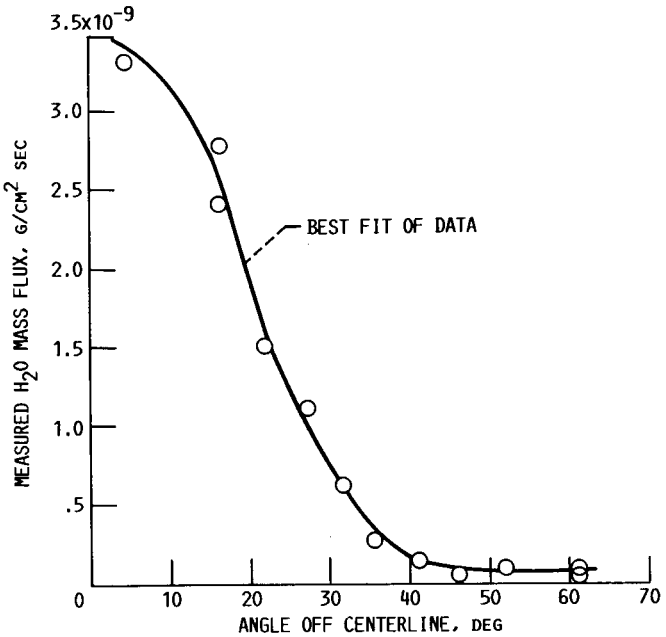

(A) MEASURED MASS FLUX AS A FUNCTION OF ANGLE OFF CENTERLINE (H_2O TRACER METHOD). AXIAL STATION IS 36.4 CM DOWNSTREAM OF THE THRUSTER EXIT PLANE.

FIGURE 9. - MEASURED H_2O MASS FLUX DATA IN THE FORWARD FLUX REGION.

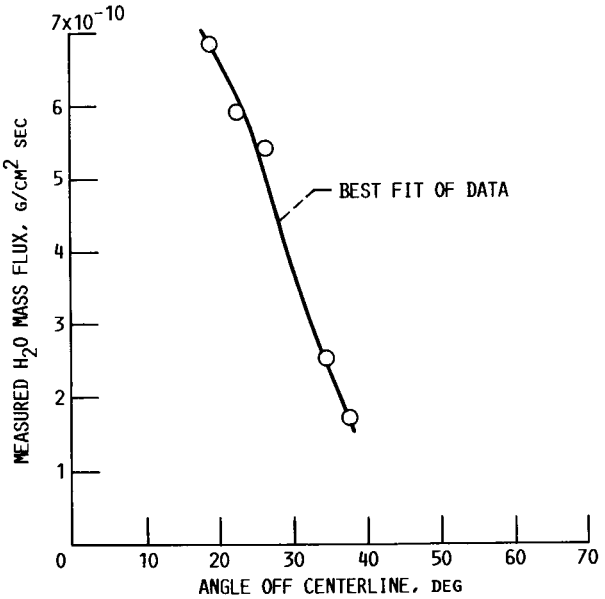

(B) MEASURED MASS FLUX AS A FUNCTION OF ANGLE OFF CENTERLINE (H_2O TRACER METHOD). AXIAL STATION IS 58.8 CM DOWNSTREAM OF THE THRUSTER EXIT PLANE.

FIGURE 9. - CONCLUDED.

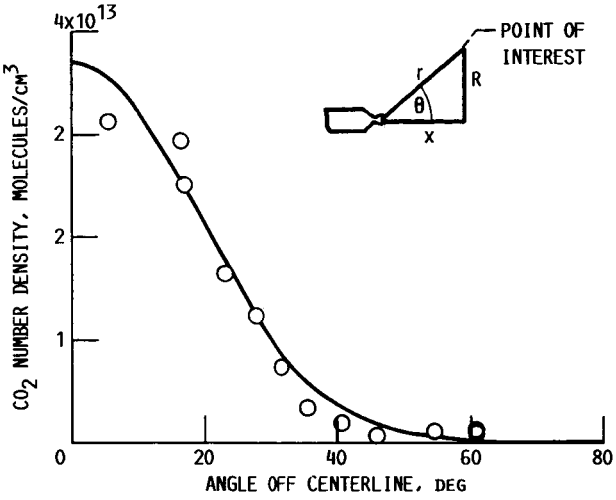

(A) CALCULATED VERSUS MEASURED CO_2 NUMBER DENSITY AS A FUNCTION OF ANGLE OFF CENTERLINE. AXIAL STATION IS 36.4 CM DOWNSTREAM OF THE THRUSTER EXIT PLANE. DATA ARE CURVE-FIT AT $\theta = 27.5^0$.

FIGURE 10. - COMPARISON OF EXPERIMENTAL DATA WITH ANALYSIS.

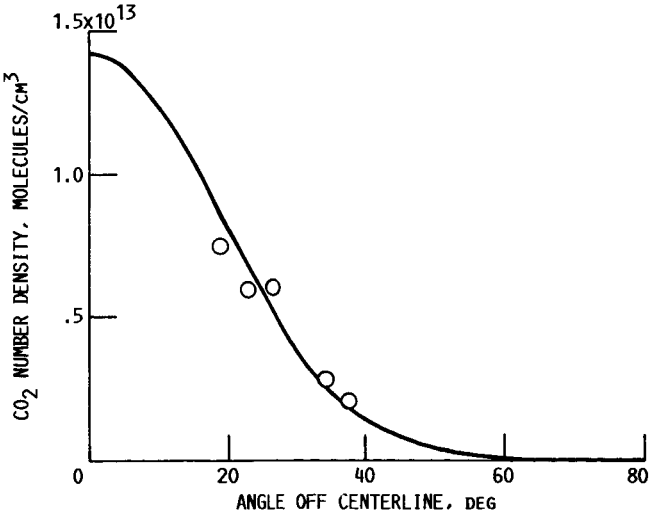

(B) CALCULATED VERSUS MEASURED Co_2 NUMBER DENSITY AS A FUNCTION OF ANGLE OFF CENTERLINE. AXIAL STATION IS 58.8 CM DOWNSTREAM OF THE THRUSTER EXIT PLANE. DATA ARE CURVE-FIT USING THE SAME CORRECTION FACTOR AS THE PREVIOUS PLOT.

FIGURE 10. - CONCLUDED.

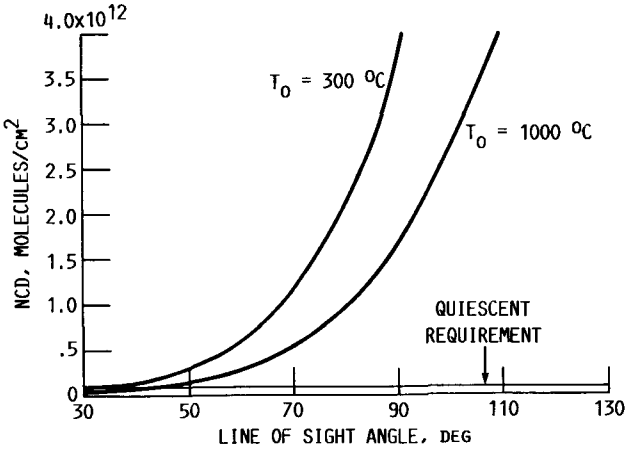

FIGURE 11. - CALCULATED NUMBER COLUMN DENSITY AS A FUNCTION OF LINE-OF-SIGHT ANGLE FOR A RESISTOJET THRUSTER USING H_2O PROPELLANT. THE OBSERVER ZENITH IS AT A L-O-S ANGLE OF 0^0 WHILE THE RESISTOJET SOURCE IS AT 145^0. THE RESISTOJET THRUST LEVEL IS 220 MN (50 MLB_F).

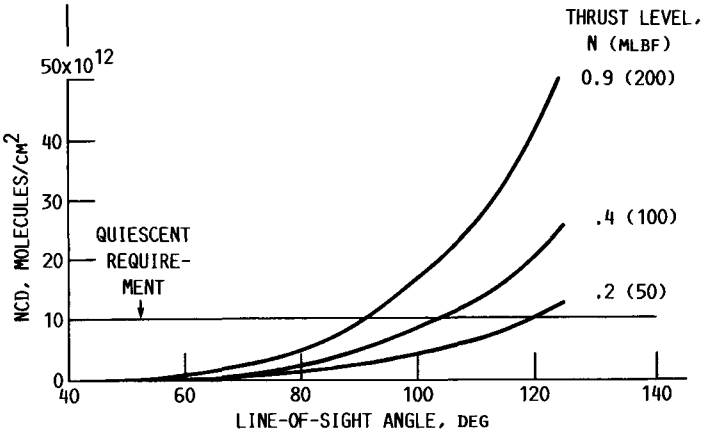

FIGURE 12. - CALCULATED NUMBER COLUMN DENSITY AS A FUNCTION OF LINE-OF-SIGHT ANGLE FOR A RESISTOJET THRUSTER OPERATING ON A BENIGN PROPELLANT MIXTURE OF H_2, N_2, HE, AND AR. THE OBSERVER ZENITH IS AT A L-O-S ANGLE OF 0^0 WHILE THE RESISTOJET SOURCE IS AT 145^0.

1. Report No.	2. Government Accession No.	3. Recipient's Catalog No.
NASA TM-88852		

4. Title and Subtitle	5. Report Date
An Analytical and Experimental Investigation of Resistojet Plumes	6. Performing Organization Code: 481-02-02

7. Author(s)	8. Performing Organization Report No.
Lynette M. Zana, David J. Hoffman, Loranell R. Breyley, and John S. Serafini	E-3243
	10. Work Unit No.

9. Performing Organization Name and Address	11. Contract or Grant No.
National Aeronautics and Space Administration Lewis Research Center Cleveland, Ohio 44135	13. Type of Report and Period Covered: Technical Memorandum

12. Sponsoring Agency Name and Address	14. Sponsoring Agency Code
National Aeronautics and Space Administration Washington, D.C. 20546	

15. Supplementary Notes

Prepared for the 25th Aerospace Sciences Meeting, sponsored by the American Institute of Aeronautics and Astronautics, Reno, Nevada, January 12-15, 1987. Lynnette M. Zana and David J. Hoffman, NASA Lewis Research Center; Loranell R. Breyley and John S. Serafini, University of Akron, Akron, Ohio 44325.

16. Abstract

As a part of the electrothermal propulsion plume research program at the NASA Lewis Research Center, efforts have been initiated to analytically and experimentally investigate the plumes of resistojet thrusters. The method of G.A. Simons for the prediction of rocket exhaust plumes is developed for the resistojet. Modifications are made to the source flow equations to account for the increased effects of the relatively large nozzle boundary layer. Additionally, preliminary mass flux measurements of a laboratory resistojet using CO_2 propellant at 298 K have been obtained with a cryogenically cooled quartz crystal microbalance (QCM). There is qualitative agreement between analysis and experiment, at least in terms of the overall number density shape functions in the forward flux region.

17. Key Words (Suggested by Author(s))	18. Distribution Statement
Exhaust plumes Contamination Space Station resistojets	Unclassified - unlimited STAR Category 20

19. Security Classif. (of this report)	20. Security Classif. (of this page)	21. No. of pages	22. Price*
Unclassified	Unclassified		

*For sale by the National Technical Information Service, Springfield, Virginia 22161